Supplementary Material for "The Charge Density Study of Urea from Synchrotron Diffraction Data"

1. Powder diffraction: Anisotropic peak broadening

The results of the fits to the powder data are summarized in table S1 while Figures S1 illustrates the fit quality.

The powder diffraction patterns display anisotropic broadening and the peak widths increase upon lowering the temperature. This is illustrated in Fig. S2A, which compares reflections (002) and (011) at 295 and 10 K. At 295 K, the peak widths are similar with (011) being slightly, but significantly, broader than (002). At 10 K, both peaks have visibly broadened, but (011) far more so than (002). This shows that, not only is there anisotropic peak broadening, but in addition, the peak widths increase in an anisotropic fashion at lower temperatures.

Five peaks were analyzed in detail using fits to asymmetric Lorentzians, $p_i(2\theta)$, that were defined by $L_{i,s}(2\theta) = w_{i,s}^2/(w_{i,s}^2+(2\theta-2\theta_i)^2)$, where

$$p_i(2\theta) = I_i \times \begin{cases} L_{i,l}(2\theta), \text{if } 2\theta < 2\theta_i \\ L_{i,r}(2\theta), \text{otherwise.} \end{cases}$$

Here $w_{i,s}$ is the half-width at half maximum of peak i on side s (left or right) of $2\theta_i$. I_i is the peak height at $2\theta_i$. In addition to p_i a constant background was refined. The total FWHM is then $w_{i,l}+w_{i,r}$. The temperature dependence of the FWHMs thus derived is presented in Fig. S2B. The increase in peak width on lowering the temperature is smallest for reflections of the type (00l) and (hh0). Reflections of the type (h0l) are the broadest at all temperatures and have the largest peak width temperature gradient.

The anisotropic peak broadening (Stephens, 1999) was Lorentzian at all temperatures. For tetragonal symmetry, only the terms S_{400}, S_{004}, S_{220} and S_{202} are allowed. The results are given in Table S1. The refined S_{HKL} follow the picture derived from the individual peak fits. Qualitative observations are summarized in Table S2.

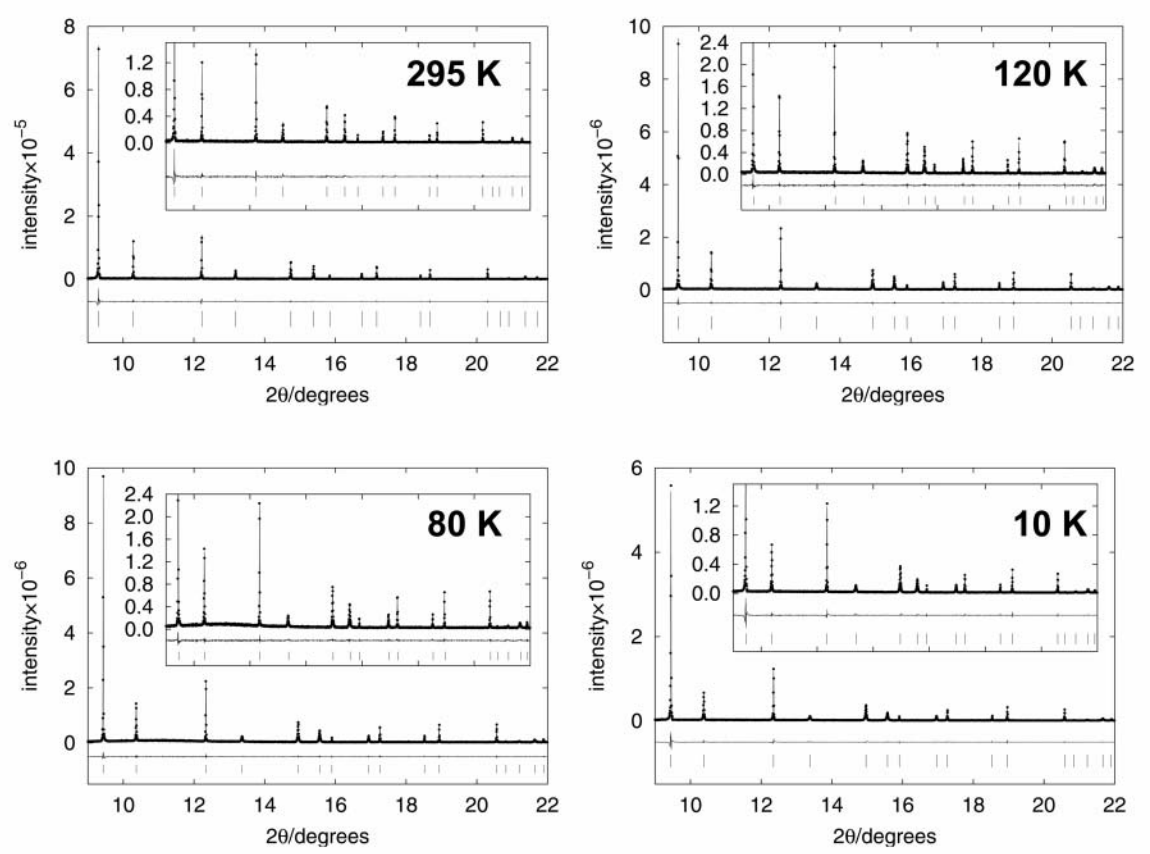

Figure 1 Le Bail fits of urea, 295, 120, 80 and 10 K. Note that the scale changes between the two plots. Tick-marks on the *x*-axis in the inset are the same as in the main plot.

Table 1 Results of Le Bail fits to urea powder patterns. The number of parameters was 46, except for 80 K where it was 45. Besides the four anisotropic profile parameters, the model consists of a 36 term linear background interpolation function, *a* and *c*, the zero point, two asymmetry parameters and, for the 295, 120 and 10 K data sets, a constant Gaussian width parameter, *W*.

T/K	295	120	80	10
Data points	2698	2698	2698	2599
wRp	0.1343	0.1150	0.0956	0.1149
Rp	0.1007	0.0810	0.0708	0.0797
χ^2	1.793	1.390	1.319	2.977
a/Å	5.64716(6)	5.57740(6)	5.56883(5)	5.56349(6)
c/Å	4.70178(4)	4.68644(4)	4.68420(4)	4.68313(5)
S_{400}	0.201(8)	0.715(16)	0.93(2)	1.38(3)
S_{004}	0.027(4)	0.072(7)	0.080(8)	0.099(13)
S_{220}	-0.101(6)	-0.428(11)	-0.571(14)	-0.87(2)
S_{202}	0.033(3)	0.024(3)	0.042(4)	0.045(5)
W	0.014(3)	0.046(3)	-	0.027(5)

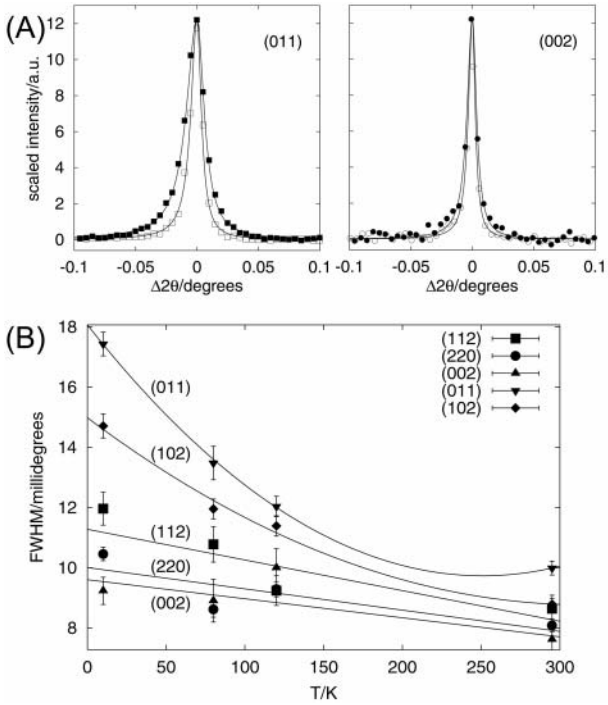

Figure 2 Temperature dependent anisotropic peak broadening in urea from the high resolution powder diffraction measurements. In A, open symbols: room temperature, closed symbols: 10 K. Note the large variation in the temperature dependence of the broadening for different reflections. The background has been subtracted and the reflections brought to the same scale, which explains the larger scatter in the experimental spectrum of (002) whose peak intensity is about 7 times lower than that of (011). Full lines represent asymmetric Lorentzian LSQ fits.

Table 2 Summary of the anisotropic strain broadening in urea.

Reflection class	width	Evolution with decreasing T
(*h*00)	broad	steep increase, second order behavior
(*h*0*h*)	broad	steep increase, second order behavior
(*hh*0)	narrow	almost flat
(*hhh*)	middle	small linear increase
(00*l*)	narrow	small linear increase

2. Charge Density Model

The parameters of the multipole model are given in Table S3. Tables S5-S8 give more details on the critical points of the multipole and periodic RHF electron densities. In Fig. S3 we show the topology of the hydrogen bonding of the four-fold acceptor oxygen while a map of the negative Laplacian in the molecular plane is given in Fig. S4. The basic feature of the topology is, as could be guessed from geometric considerations, governed by the hydrogen bonds. The hydrogen bonds are situated on intersecting planes parallel to (110) and $(1\bar{1}0)$ (Swaminathan *et al.*, 1984). The

topology in the neighbourhood of the oxygen is shown in Fig. S3. The intersection of the (110) and $(1\bar{1}0)$ planes is characterized by the presence of the N-H1···O hydrogen bonds, but also by an N···N interaction. The hydrogen bonds N-H2···O, that create tapes parallel to the *c*-axis, form a ring (C-N-H2···O···H2-N-C), the ring critical point being R1 in Table S6. Two additional rings are created by the hydrogen bonds and the short N···N interactions. The first, R2 in Table S6, is given by (N-H1···O···H2-N···N), while the other, R3, is (N···N-C-N···N). These three unique rings form a cage, the critical point of which is C1. The cage is constituted by one ring of type R1, one R3, and two R2 rings (Fig. S3).

Table S9 gives an overview of literature values for the dipole moment of the urea molecule.

Table 3 Multipole parameters. The monopole parameters (P_c+P_v) are scaled to give a neutral unit cell. The quadrupole (Q) and octopole parameters (O) are scaled by 10. The hexadecapole parameters (H) are scaled by 100. For numerical accuracy, all s.u.'s are given with two digits.

	κ/Å^{-1}	α/Å^{-1}	P_c+P_v	P_c	
C	0.9914(39)	5.087(97)	6.069(41)	2.0592(30)	
O	0.9784(16)	9.10(64)	8.406(21)	P_c(C)	
N	1.0016(34)	7.24(21)	7.041(48)	P_c(C)	
H1		4.379(52)	0.859(22)		
H2		α(H1)	0.863(21)		
	D1	D3	Q1	Q3	Q5
C		0.0173(92	0.701(31)		1.090(39)
O		0.0709(68)	0.141(14)		-0.156(15)
N	0.005(11)	-0.0157(77)	0.071(13)	0.138(25)	0.012(20)
H1	-0.197(14)	-0.0875(89)	0.185(38)	0.325(87)	-0.405(54)
H2	0.0059(67)	0.222(13)	-0.069(49)	0.232(54)	0.895(77)
	O1	O3	O5	O7	
C		-0.807(82)		0.328(33)	
O		0.0188(99)		-0.0066(16)	
N	0.0081(25)	0.150(23)	-0.0090(20)	-0.0369(46)	
	H1	H3	H5	H7	H9
C	-0.439(70)		-0.051(45)		-0.110(61)
O	-0.0137(44)		0.0012(30)		0.0086(36)
N	-0.0158(54)	-0.038(17)	0.0099(54)	-0.0139(69)	0.0195(55)

Table 4 Interatomic distances and angles in urea. The neutron results cited are the 123 K SCM values uncorrected for thermal motion. Distances in Å and angles in degrees. Symmetry operations are (i) = 1-*y*,1+*x*,1-*z* and (ii) = *x*,*y*,*z*-1.

bond lengths (Å) and angles (degrees)				
		present	neutron	
	C-O	1.2565(5)	1.258(1)	
	C-N	1.3384(4)	1.341(1)	
	N-H1	1.005(2)	1.007(2)	
	N-H2	1.0020(15)	1.000(2)	
	O-C-N	121.49(2)	121.5(1)	
	N-C-N	117.02(3)	117.0(1)	
	C-N-H1	119.16(12)	119.0(1)	
	C-N-H2	120.78(13)	120.8(1)	
	H1-N-H2	120.06(17)	120.2(2)	
Hydrogen bond distances (Å) and angles (degrees)				
	N-H1···O^{i}		N-H2···O^{ii}	
	present	neutron	present	neutron
N···O	2.9941(5)	2.998(1)	2.9593(7)	2.960(1)
H···O	2.007(2)	2.009(2)	2.0644(18)	2.067(2)
N-H···O	166.86(17)	166.8(2)	147.56(18)	147.6(2)

Table 5 Intermolecular bond critical points in crystalline urea. *D* is the bond length, A···B, *D*1 is the distance from A to the BCP while *D*2 is the B-BCP distance. $\rho(\mathbf{r}_c)$ is in eÅ^{-3} while $\nabla^2\rho(\mathbf{r}_c)$, λ_1, λ_2, and λ_3 are in eÅ^{-5}. First line: present study, second line: periodic RHF 6-21G(d,p), third line: periodic RHF 6-31G(d,p), fourth line: periodic RHF 6-311G(d,p), fifth line: experimental density of ZSTVF.

	D/Å	D1/Å	D2/Å	$\rho(\mathbf{r}_c)$	$\nabla^2\rho(\mathbf{r}_c)$	λ_1	λ_2	λ_3	ε
H1···O	2.007(2)	0.739(3)	1.269(3)	0.131(3)	1.89(5)	-0.71(2)	-0.58(3)	3.175(13)	0.23(7)
	2.009	0.695	1.315	0.150	1.92	-0.72	-0.70	3.35	0.022
	2.009	0.708	1.301	0.145	1.63	-0.64	-0.60	2.87	0.071
	2.009	0.709	1.300	0.138	2.04	-0.63	-0.58	3.25	0.087
	2.014		1.269	0.159	1.58	-0.62	-0.57	2.77	0.09
H2···O	2.0644(18)	0.782(5)	1.286(5)	0.1317(19)	1.525(14)	-0.677(13)	-0.670(8)	2.87(3)	0.01(2)
	2.067	0.752	1.315	0.127	1.91	-0.60	-0.58	3.09	0.031
	2.067	0.764	1.303	0.125	1.55	-0.51	-0.49	2.55	0.036
	2.067	0.758	1.309	0.118	1.90	-0.49	-0.47	2.86	0.041
	2.071		1.275	0.142	1.53	-0.53	-0.52	2.58	0.02
N···N	3.4603(7)	1.701(14)	1.762(14)	0.0184(3)	0.404(3)	-0.0541(6)	-0.0331(10)	0.491(5)	0.64(5)
	3.461	1.699	1.762	0.023	0.48	-0.07	-0.025	0.57	1.657
	3.461	1.680	1.786	0.027	0.36	-0.06	-0.031	0.46	1.042
	3.461	1.684	1.782	0.026	0.38	-0.06	-0.014	0.46	3.438
N···N	4.2800(7)	2.1477(15)	2.1477(15)	0.0043(2)	0.0675(12)	-0.0091(2)	-0.0082(3)	0.0848(16)	0.11(5)
	4.284	2.142	2.142	0.002	0.07	-0.01	-0.00[a]	0.08	7.061
	4.284	2.142	2.142	0.005	0.11	-0.01	-0.01	0.12	0.642
	4.284	2.142	2.142	0.006	0.10	-0.01	-0.01	0.11	0.543

[a] The value of λ_2 is non-zero but very small, -0.0006 eÅ^{-3}.

Table 6 Fractional coordinates of the bond critical points in urea. First line: present study; second line: periodic HF, 6-21G(d,p); third line: periodic HF, 6-31G(d,p); fourth line: periodic HF, 6-311G(d,p). The periodic HF calculations were performed at the neutron geometry.

	x	*y*	*z*	Pos	interaction
1	0.4050(9)	0.0950(9)	0.1806(10)	4c	H2···O
	0.41261	0.08739	0.16497		
	0.41166	0.08834	0.16908		
	0.41171	0.08829	0.16749		
2	0.1536(4)	0.3465(4)	0.6769(15)	4c	H1···O
	0.15942	0.34058	0.67687		
	0.15789	0.34211	0.67529		
	0.15763	0.34237	0.67645		
3	0.0	0.5	0.4266(7)	2c	C-O
	0.0	0.5	0.41978		
	0.0	0.5	0.41534		
	0.0	0.5	0.41774		
4	0.4416(6)	0.0584(6)	0.7327(9)	4c	C-N
	0.44937	0.05063	0.72497		
	0.45175	0.04825	0.72255		
	0.44983	0.05017	0.72450		
5	0.27256(19)	0.22744(19)	0.7414(3)	4c	N-H1
	0.27129	0.22871	0.74119		
	0.26887	0.23113	0.73885		
	0.27065	0.22935	0.74049		
6	0.35635(5)	0.14365(5)	0.9807(4)	4c	N-H2
	0.35664	0.14336	0.98253		
	0.35675	0.14325	0.98738		
	0.35676	0.14324	0.98394		
7	0.899(3)	0.758(3)	-0.014(3)	8f	N···N
	0.89212	0.75148	-0.00752		
	0.89098	0.76772	-0.00121		
	0.89305	0.76728	-0.00386		
8	0	0	0.218(4)	4d	N···N
	0	0	0.18428		
	0	0	0.17490		
	0	0	0.17240		

Table 7 Ring and cage critical points in the experimental electron density of urea. The column 'pos' specifies the multiplicity and Wyckoff letter of the position. $\rho(\mathbf{r}_c)$ is in *e*Å-3 while $\nabla^2\rho(\mathbf{r}_c)$, λ_1, λ_2, and λ_3 are in *e*Å^{-5}.

	x	*y*	*z*	pos	$\rho(\mathbf{r}_c)$	$\nabla^2\rho(\mathbf{r}_c)$	λ_1	λ_2	λ_3
R1	0.5	0.0	0.0661(7)	2c	0.0322(12)	1.186(8)	-0.103(6)	0.538(11)	0.748(7)
R2	0.430(3)	0.772(3)	0.092(3)	8f	0.0170(4)	0.444(4)	-0.0566(10)	0.0506(17)	0.450(5)
R3	0.1721(11)	0.3279(11)	0.025(3)	4e	0.0140(5)	0.372(4)	-0.045(2)	0.0582(19)	0.359(6)
R4	0.069(3)	0.029(3)	0.107(5)	8f	0.0032(1)	0.0722(9)	-0.0055(4)	0.0258(5)	0.0519(7)
R5	0.112(5)	0.055(5)	0.271(7)	8f	0.0033(1)	0.0570(7)	-0.0075(5)	0.0113(6)	0.0532(11)
R6	0.130(3)	0.118(3)	0.428(6)	8f	0.0026(2)	0.0665(12)	-0.0091(2)	0.0184(12)	0.0572(9)
C1	0.1287(11)	0.3713(11)	0.939(2)	4c	0.0114(6)	0.386(4)	0.0699(19)	0.083(3)	0.233(8)
C2	0.0	0.0	0.5	2b	0.0013(2)	0.0218(12)	0.0072(4)	0.0072(4)	0.0075(3)
C3	0.0	0.0	0.0	2a	0.0025(1)	0.0527(8)	0.0083(3)	0.0222(4)	0.0222(4)
C4	0.116(6)	0.054(6)	0.173(8)	8f	0.0030(1)	0.0828(9)	0.0068(4)	0.0247(10)	0.0513(7)
C5	0.2366(9)	0.2634(9)	0.407(8)	4c	-0.0008(2)	0.1655(18)	0.0245(5)	0.032(3)	0.109(3)

Table 8 Ring and cage critical points in the *ab initio* periodic RHF electron density of urea. The column 'pos' specifies the multiplicity and Wyckoff letter of the position. $\rho(\mathbf{r}_c)$ is in *e*Å-3 while $\nabla^2\rho(\mathbf{r}_c)$, λ_1, λ_2, and λ_3 are in *e*Å^{-5}.

	x	*y*	*z*	pos	$\rho(\mathbf{r}_c)$	$\nabla^2\rho(\mathbf{r}_c)$	λ_1	λ_2	λ_3
R1	0.5	0.0	0.0767	2c	0.0512	1.262	-0.175	0.710	0.727
	0.5	0.0	0.0713		0.0541	1.056	-0.161	0.484	0.733
	0.5	0.0	0.0727		0.0536	0.989	-0.154	0.497	0.646
R2	0.4241	0.7872	0.0968	8f	0.0216	0.478	-0.063	0.056	0.485
	0.4220	0.7802	0.0939		0.0247	0.445	-0.064	0.065	0.444
	0.4197	0.7686	0.0818		0.0252	0.420	-0.066	0.027	0.459
R3	0.1778	0.3222	0.0518	4e	0.0187	0.430	-0.021	0.067	0.384
	0.1786	0.3214	0.0457		0.0214	0.356	-0.023	0.071	0.309
	0.1848	0.3152	0.0687		0.0208	0.351	-0.025	0.060	0.316
R4	0.0277	0.0118	0.1798	8f	0.0018	0.072	-0.005	0.001	0.076
	0.0512	0.0189	0.1420		0.0047	0.107	-0.010	0.013	0.103
	0.0517	0.0183	0.1373		0.0054	0.099	-0.009	0.014	0.095
R5'	0.2546	0.2454	0.3448	4e	0.0052	0.120	-0.013	0.024	0.108
	0.2453	0.2547	0.3354		0.0070	0.141	-0.008	0.016	0.133
	0.2446	0.2554	0.3336		0.0078	0.146	-0.008	0.019	0.135
C1	0.1336	0.3665	0.9444	4e	0.0169	0.425	0.048	0.084	0.293
	0.1388	0.3612	0.9499		0.0198	0.384	0.049	0.079	0.257
	0.1439	0.3561	0.9639		0.0194	0.376	0.030	0.084	0.262
C2	0.0	0.0	0.5	2b	0.0003	0.010	0.002	0.004	0.004

	0.0	0.0	0.5		0.0006	0.020	0.006	0.007	0.007
	0.0	0.0	0.5		0.0009	0.022	0.007	0.007	0.007
C3	0.0	0.0	0.0	2a	0.0012	0.051	0.004	0.024	0.024
	0.0	0.0	0.0		0.0036	0.096	0.009	0.043	0.044
	0.0	0.0	0.0		0.0044	0.090	0.009	0.040	0.040

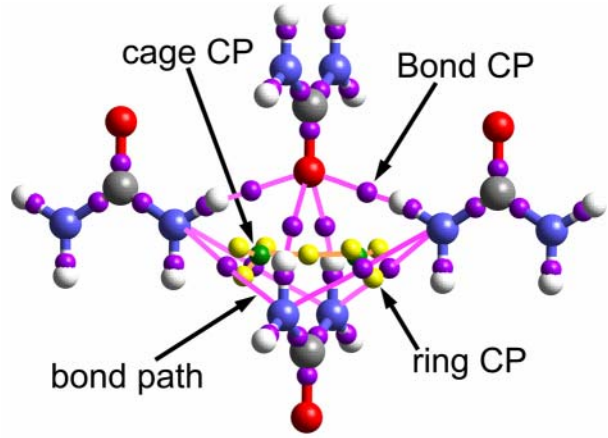

Figure 3 Critical points and bond paths of urea: the hydrogen bonded cluster.

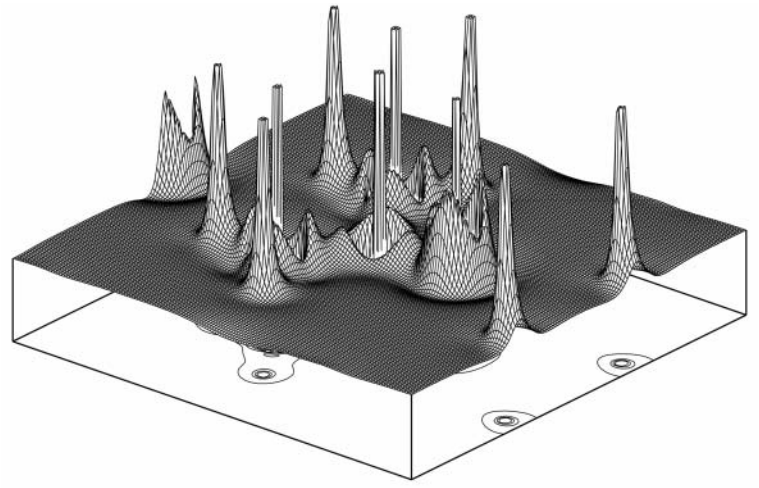

Figure 4 The negative of the Laplacian of the charge density of urea, $-\nabla^2\rho(\mathbf{r})$.

Table 9 Dipole moment of urea: values from the literature. The dipole moment is in all cases given with the number of significant digits reported in the original publication.

μ/D	solvent	temperature	method	Reference
4.56	H_2O	Ambient	Not detailed clearly	Kumler & Fohlen (1942)
5.68	H_2O	Ambient	Dielectric increment	Gäumann (1958)
4.56	Dioxane	Ambient	Dielectric increment	Gäumann (1958)
4.66	Polyether	Ambient	Dielectric increment	Gäumann (1958)
6.38	Butylcellosolve	Ambient	Dielectric increment	Gäumann (1958)[(a)]
6.30	Methylcellosolve	Ambient	Dielectric increment	Gäumann (1958)[(a)]
4.38	Acetone	Ambient	Dielectric increment	Gäumann (1958)
4.51	Ethanol	Ambient	Dielectric increment	Gäumann (1958)
5.06	Methanol	Ambient	Dielectric increment	Gäumann (1958)
4.20	H_2O	Ambient	Dielectric increment	Gilkerson & Srivastava (1960)
6.25	20% w/w H_2O/acetone	Ambient	Dielectric increment	Gilkerson & Srivastava (1960)
3.83(4)	gas phase	80-90ºC	Microwave Stark effect	Brown, Godfrey & Storey (1975)
5.79, 4.83	H_2O	Ambient	Kerr effect	Aroney *et al*. (1988)[(b)]

[(a)] cellosolve: ethylene glycol mono alkyl ether, where the alkyl contains one to four carbons, the prefix given in the table gives the name of the alkyl.

[(b)] The two values are derived from the same experiment but using two different models for the local static solvent field.

References for supplementary material

Aroney, M. J.; Dowling, K. M.; Patsalides, E.; Pierens, R. K. & Filipczuk, S. W. (1988). *J. Chem. Soc. Faraday Trans. 1* **84**, 4169-4179.

Brown, R. D.; Godfrey, P. D. & Storey, J. (1975). *J. Mol. Spec*. **58**, 445-450.

Gäumann, T. (1958). *Helv. Chim. Acta* **41**, 1956-1970.

Gilkerson, W. R. & Srivastava, K. K. (1960). *J. Phys. Chem*. **64**, 1485-1487.

Kumler, W. D. & Fohlen, G. M. (1942). *J. Am. Chem. Soc*. **64**, 1944-1948.

Stephens, P. W. (1999). *J. Appl. Cryst*. **32**, 281-289.

Swaminathan, S., Craven, B. M. & McMullan, R. K. (1984). *Acta Cryst*. B**40**, 300-306.